Journal of Hydrology (NZ) 42 (2): 101-112, 2003

Assessment of a radar-based nowcasting model for the Auckland region

H. R. Larsen and W. R. Gray
National Institute for Water and Atmospheric Research
PO Box 14-901, Wellington, New Zealand

Abstract

A model for extrapolating weather radar data to provide short-term rainfall forecasts is assessed for two catchments near Auckland, New Zealand. The forecasts are made using a technique that assumes decay of the small spatial scale components of the precipitation pattern, as these tend to be short-lived. At the same time the remaining, larger-scale components are translated with the storm motion. Results from applying the technique to representative frontal rain events show that the pattern of reflectivity is well forecast, with few timing errors and little bias in catchment averages. A simple estimate of forecast skill shows this technique is an improvement over catchment forecasts made assuming persistence. The larger the catchment, the more accurate are the forecasts.

Introduction

Weather radar is increasingly being looked to as a source of input data for short-term rainfall forecasting ("nowcasting") because it offers real-time, remote, centralized monitoring of precipitation over large areas of complex terrain, over which the precipitation can be highly variable. The accuracy with which short-term future rainfall rates can be estimated from these radar-derived data is therefore increasingly important.

A radar-based rainfall nowcasting model for use in New Zealand has been developed and evaluated for the Auckland region. The system has been used to provide forecasts of catchment rainfall up to 1.5 hours in advance, but longer forecasts can be made. Depending on the speed of the storm system, forecasts of up to three hours in advance are quite feasible. Such forecasts can be valuable for urban and rural flood control, for example, and in other hydrological forecasting. Because the radar input is more spatially extensive than measurements from isolated raingauges and provides information on the highly variable small-scale pattern of the rainfall that is not available from the gauges, the radar-based nowcasts may offer more accurate estimates and forecasts of catchment rainfall for hydrological modelling. The availability of high spatial resolution, short-term forecasts is also useful for industrial scheduling, the management of outdoor sports venues, and similar rain-sensitive activities.

Radar nowcasting has two components: the generation of forecasts of what the future radar measurements will be like and, secondly, the conversion of the radar measurements (or forecast measurements) to rainfall values. Weather radar detects the reflection of radar signals by the precipitation in the radar beam. The radar measures a property of the precipitation called its radar

reflectivity. This is closely related to the rainfall rate, and increasing radar reflectivity can be interpreted as increasing rainfall. But it is not a direct measurement of rainfall rate and, because the beam is some distance above the ground, it does not necessarily represent what is happening at the surface. The relationship between the radar observations aloft and the true surface rainfall has been addressed elsewhere (e.g., Austin, 1987).

We focus here on the first component: the nowcasting model and the relationship between the forecast of what the radar will observe at some future time and what the radar actually does observe at that time. After describing briefly the operation of the radar and how the nowcasts are generated, we look at two case studies of rain events and the accuracy of forecasts made for these events for various catchments.

Data

The data used in this study come from an Ericsson C-band weather radar operated by the Meteorological Service of New Zealand Ltd at Warkworth, near Auckland. The radar measures reflectivity in the hemisphere over the radar out to a range of 240 km, once every 15 minutes.

The reflectivity is measured during a circular scan with a slightly elevated beam. The range resolution of the data is 2 km and the angular resolution in azimuth is 0.86°. Because the beam is not horizontal and because of the curvature of the earth, the measurements are made not at the surface but at increasingly higher elevations as the range from the radar increases. At the lowest beam elevation used, 0.5°, the height of the centre of the beam is 1.5 km at 120 km, rising to 6 km at the maximum range of 240 km. During a scanning cycle (which takes two minutes) a series of scans are made at increasing elevation angle, to provide data for as much as practicable of the hemisphere above the radar. A horizontal slice through these data at some height then provides a map of radar reflectivity at that height in the atmosphere (Fig. 1).

Figure 1 was generated using data from the Auckland radar for 00h00 on 01 July 1998. The circular area in the top left image is the plot of radar reflectivity around the radar. The data are from approximately 1.5 km height out to a range of 120 km. Beyond 120 km the radar data are from the lowest radar scan and so rise to 6 km at 240 km. Some of the structure observed in the map at ranges beyond 120 km may be due to this change in elevation across the map and could reflect the vertical structure of the precipitation field rather than its horizontal structure.

Nowcasting model operation

Weather radars typically provide a series of such maps of radar reflectivity at 5- to 30-minute intervals. A number of techniques have been used to extrapolate this time series of maps to provide reflectivity forecasts, under the assumption that there is no significant change in the general behaviour of the precipitation pattern. Typically the techniques involve deriving a displacement vector for the reflectivity pattern between successive maps, interpreting this as a movement vector over the time interval, and advancing the latest map accordingly (Ligda, 1953; Austin and Bellon, 1974). To allow for the relative movement of different precipitation areas, some techniques differentiate between small, high-intensity parts of the pattern and the larger, low-intensity areas, interpreting them as convective precipitation cores and widespread rain respectively, and determine different movement vectors for the two precipitation types (e.g., Bremaud and Pointin, 1993). Others divide the area mapped by the radar into smaller sub-areas and derive independent motion vectors for each sub-area (Bellon *et al.*, 1980; Seed, 2003). Still others attempt to "develop" the pattern, as well as translate it, in order to

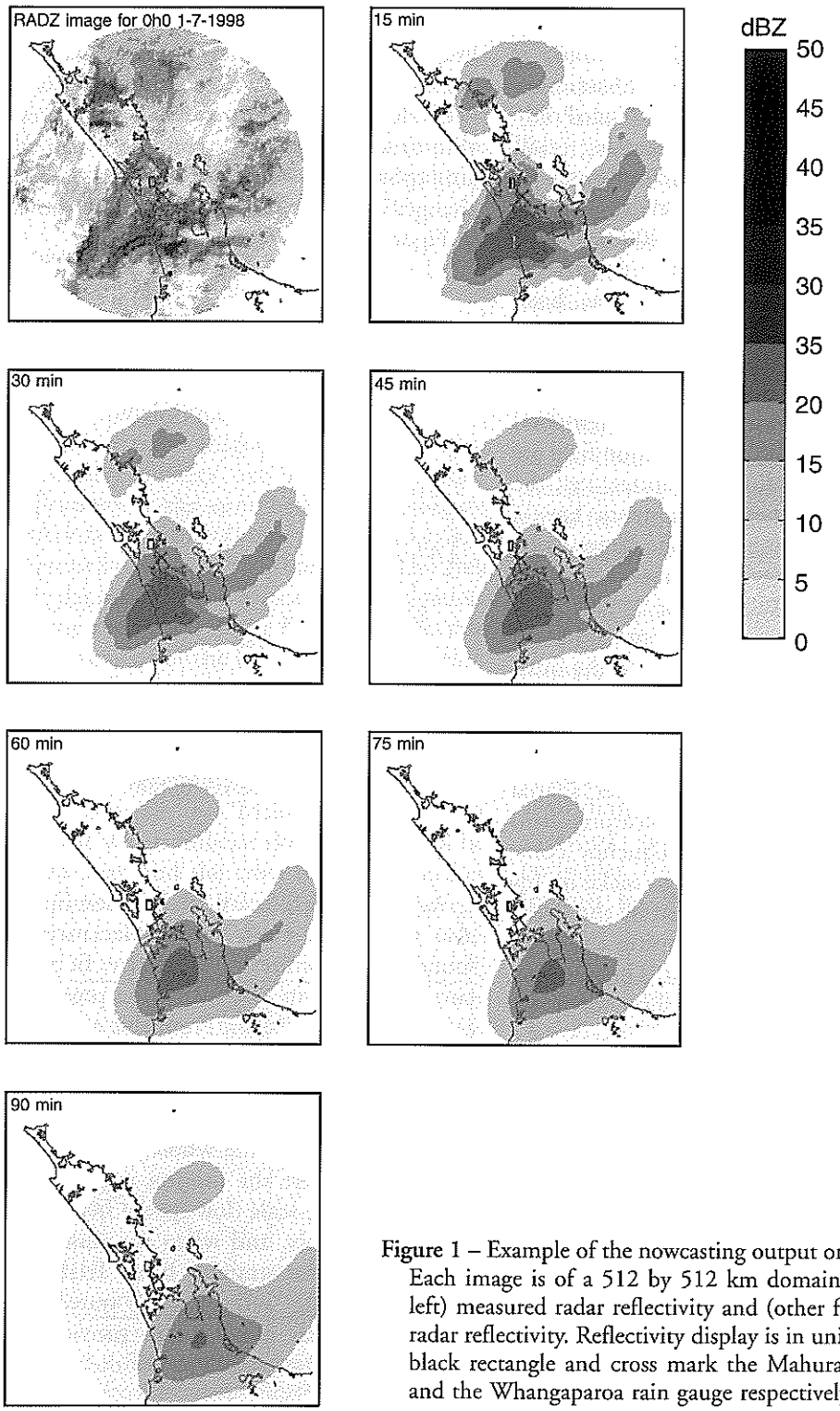

Figure 1 – Example of the nowcasting output on 01 July 1998. Each image is of a 512 by 512 km domain, showing (top left) measured radar reflectivity and (other frames) forecast radar reflectivity. Reflectivity display is in units of dBZ. The black rectangle and cross mark the Mahurangi catchment and the Whangaparoa rain gauge respectively.

reflect the observed changes in the preceding periods (Pierce *et al.*, 2000; Mecklenburg *et al.*, 2000). By and large most of these more sophisticated techniques have produced only a limited increase in forecasting skill compared with methods that simply assume that the current pattern persists and is translated (Smith and Austin, 2000).

An algorithm for generating short-term forecasts from the radar data has been developed in association with NIWA by collaborators at the Australian Bureau of Meteorology. This nowcasting algorithm is based on the observation that the temporal and spatial scales of the precipitation field are related, so that small-scale features, i.e., the high spatial frequency components, have a much shorter lifetime than the larger-scale, low spatial frequency components (Kessler and Russo, 1963; Wilson *et al.* 1998). Thus the large-scale features of the precipitation field may persist from one time to the next, e.g., from the radar observation time to the forecast time, while the small-scale features may not. The nowcasting algorithm produces a forecast by allowing the higher spatial frequency components in the measured field to decay, while the lower frequency components are amplified a little to make up for the loss of precipitation caused by the decay of the high frequencies, keeping the total precipitation amount constant. The resulting forecast field is translated to allow for storm movement.

The resulting forecast must be interpreted as a best estimate, in the statistical sense, of the reflectivity at the forecast time. At the later time the true precipitation field will again have small-scale features present, features which are not present in the "smoothed" forecast. These, however, will be new features that are independent of the small-scale features present at the earlier time and whose location and characteristics therefore cannot be forecast from these earlier features.

The rate at which the high spatial frequencies decay is determined dynamically from the correlation between earlier measured fields, for each spatial frequency. It will vary with time as the synoptic conditions and the atmospheric processes operating in the storm change. Typical correlation values are shown in Figure 2.

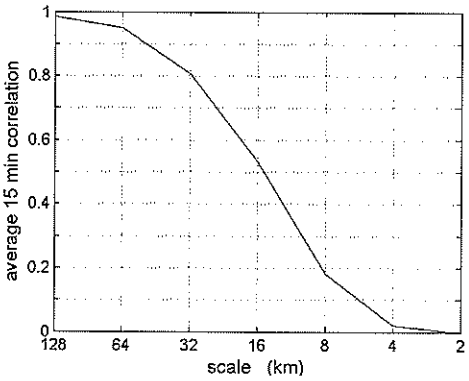

Figure 2 – The correlation between the various spatial scale components of successive radar maps, 15 minutes apart, averaged over a four-hour period centred on 00h00 on 01 July 1998.

As noted, the forecast precipitation field is also translated. First, the displacement is found that maximizes a least-squares fit of the current reflectivity map with the preceding one, 15 minutes earlier. From this a velocity vector is derived and used to move the forecast fields. In the current study, a single motion vector is derived (at each observation time) and used for the whole field. This is satisfactory where the motion is essentially that of the large-scale (low spatial frequency) components only, and when the motion is essentially in a straight line. Trials are underway using independent translation vectors for each quadrant to provide for rotation as well as translation of the forecast field (Seed, 2001).

The forecast scheme does not allow for any development (growth or decay) of the large-scale rain field, as existing nowcasting techniques that incorporate development have not produced an improvement in the forecasts commensurate with the complexity introduced (Smith and Austin, 2000).

Nowcasting output

The nowcasting algorithm has been used to generate case study sets of radar and associated nowcast data (Fig. 1).

As noted, the top left image is the plot of radar reflectivity around the radar at a nominal 1.5 km height (higher beyond 120 km). Successive images are maps of forecast reflectivity at the same height at 15-minute intervals from 00h00 out to 01h30, i.e., for forecast intervals up to 90 minutes. The grey circular area of radar/forecast coverage moves during the period of the forecasts at the rate of movement of the large-scale precipitation features (to the south-east in Figure 1), reflecting the fact that no forecast information is available outside this area.

The small rectangle near the centre of each map delineates the "Mahurangi" catchment area for which forecast skill statistics will be given later, and the cross below it indicates the location of the Whangaparoa rain gauge.

Cases studied

Two precipitation events from 1998 will be examined here; the events covered the periods 30 June–01 July and 17–18 August 1998. Both events involved travelling frontal systems producing widespread moderate rain crossing the North Auckland region: synoptic weather charts show they were associated with low-pressure systems to the northwest of New Zealand (Fig. 3). Twenty-four-hour rainfall recorded at Whangaparoa (near the radar) for the events were 9.0 mm and 8.8 mm respectively.

In such conditions, New Zealand's location in the South-West Pacific ensures the ready availability of warm moist sub-tropical ocean air to feed down from the north, around the low-pressure area and into the frontal system. Such frontal systems are thus some of the principal sources of significant rain episodes in New Zealand and hence one of the primary targets of a nowcasting system.

Forecasts of catchment rain rate

To test the performance of the nowcasting algorithm, the measurements averaged over a specified surface catchment area at a particular time were compared with the forecast for the same time and area. The

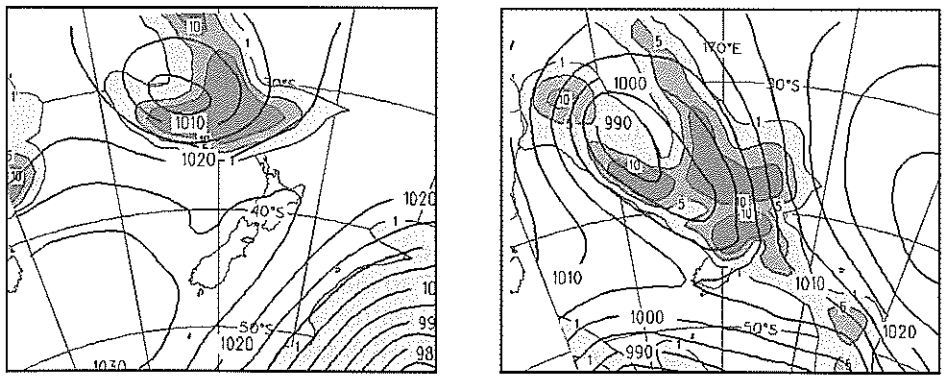

Figure 3 – Barometric pressure (MSL) charts for 00h00 NZST on 01 July and 06h00 on 18 August 1998 (from Bracknell Fine-Mesh analysis). Estimated 6-hour rain totals from the model are shaded.

nowcasting algorithm generates maps of forecast radar reflectivity, but the end-users of these data commonly require information on rainfall rate. To make the evaluation of the performance easier to interpret, the data have therefore been transformed to a "nominal rain rate", to reflect an appropriate relative weighting, before integration over the catchments. For any particular observation the transformation between reflectivity and rain rate depends on variables such as the sizes of the raindrops in the rain, which are generally not known. We have used the "standard" conversion (Marshall and Palmer, 1948):

$$R = (Z/200)^{(1/1.6)}$$

which will result in a transformation that at least approximately weights the data correctly for most precipitation events. We have used this transformation and refer to the transformed data as "rain rate", but the true rain rate may differ from this by a factor of two or three, and possibly by as much as five.

For each storm, two test locations were chosen: the Mahurangi catchment area, some 15 km southwest of the radar, and an area round the Whangaparoa rainfall station, some 30 km south-southeast of the radar. The Mahurangi catchment feeds the Mahurangi River and is intensively instrumented for hydrological studies. It is also of a size (approximately 64 km^2) that is relevant for urban hydrology and for other studies of areas within New Zealand's rather variable terrain. The catchment is approximately rectangular and is represented in the radar field by the 7 km by 15 km rectangular area outlined in Figure 1.

Time series of measured and representative forecast rainfall for the Mahurangi catchment for the storm on 30 June–01 July 1998 show the forecasts are generally reasonable, particularly for the major rain periods, which are forecast well in both time and magnitude (Fig. 4). Rain is not forecast for the no-rain

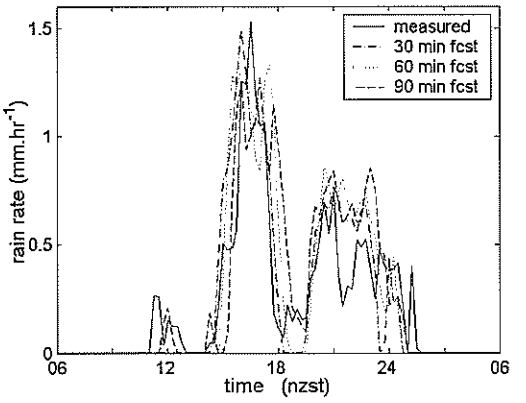

Figure 4 – Rainfall rates measured and forecast (for periods of 30, 60 and 90 minutes ahead) for the Mahurangi catchment, for the 24-hour period from 06h00 on 30 June to 06h00 on 01 July 1998.

periods before and after the storm. The first major rain period (around 17h on the 30th) was delayed in the 90-minute and, to a lesser extent, the 60-minute forecasts, and (as might be anticipated for smoothed fields) the forecasts underestimate its maximum intensity somewhat. The forecasts overestimate the intensity of the latter part of the second rain period, and this leads to an overestimation of the rain accumulation in the catchment for the 24-hour period (Fig. 5). In practice, the observed data would be used in real time to correct the forecast accumulation, so any errors would never be greater than those occurring over the 90-minute forecast interval from the current time.

The correlation between the measured and forecast rainfall during this first event, averaged over the Mahurangi catchment, declines as the forecast interval increases from 30 to 60 and to 90 minutes (Fig. 6).

For the second storm studied, occurring on 17–18 August 1998, the analysis has focussed on rainfall near the Whangaparoa rainfall station on the Whangaparoa peninsula, some 30 km south-southeast of the radar. Time

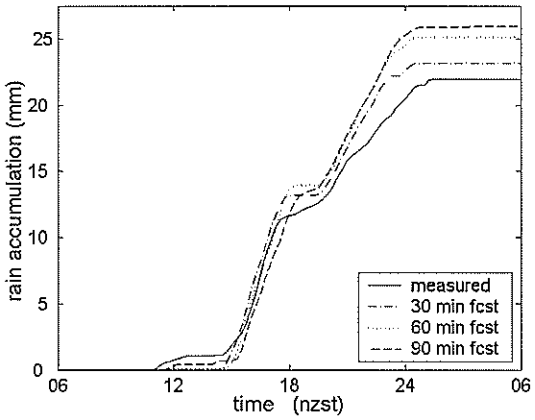

Figure 5 – Rainfall accumulation measured and forecast (for periods of 30, 60 and 90 minutes ahead) for the Mahurangi catchment, for the 24 hour period from 06h00 on 30 June to 06h00 on 01 July 1998.

series for an imaginary catchment with an area of 64 km^2 (comparable with the Mahurangi catchment) again show the forecast of the main heavy-rain event is generally good (Fig. 7). There are no obvious timing or magnitude errors except around 06h00, when significantly increased rainfall was forecast for 60 minutes and 90 minutes ahead at a time, but the rainfall actually decreased for a short period. These errors led to an uncorrected forecast total accumulation 128% of that observed for the 24 hours (Fig. 8).

Scatter plots of the measured versus forecast rainfall, averaged over the 64 km^2 Whangaparoa catchment, for all observations during this second event again suggest that

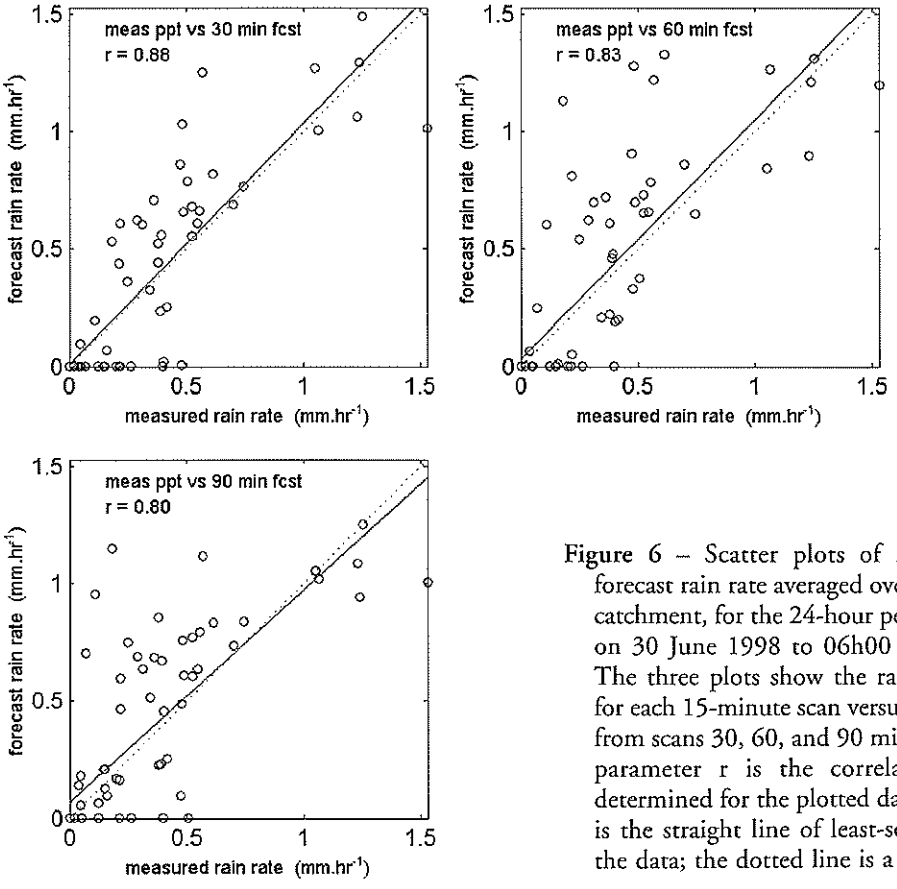

Figure 6 – Scatter plots of measured versus forecast rain rate averaged over the Mahurangi catchment, for the 24-hour period from 06h00 on 30 June 1998 to 06h00 on 1 July 1998. The three plots show the rain rate measured for each 15-minute scan versus the rate forecast from scans 30, 60, and 90 minutes earlier. The parameter r is the correlation coefficient determined for the plotted data. The solid line is the straight line of least-squares best fit to the data; the dotted line is a 1:1 line.

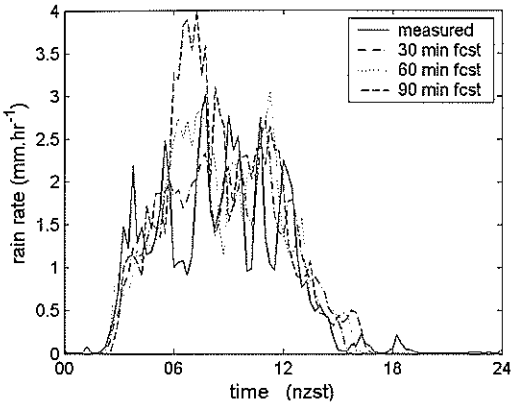

Figure 7 – Rain rates measured and forecast (for periods of 30, 60 and 90 minutes ahead) for a 64 km^2 catchment centred on Whangaparoa, for the 24 hours of 18 August 1998.

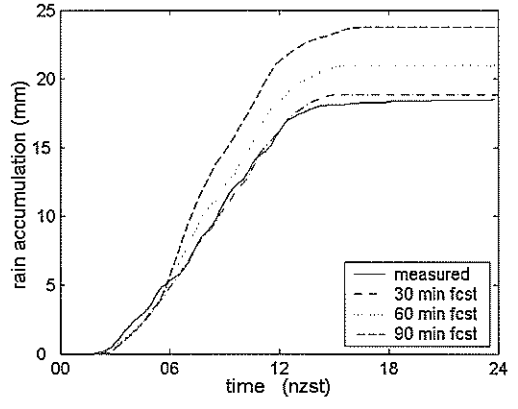

Figure 8 – Rainfall accumulation measured and forecast (for periods of 30, 60 and 90 minutes ahead) for the 64 km^2 Whangaparoa catchment, for the 24-hour period from 00h00 on 18 August 1998.

useful forecasts are being generated, but show a decrease in correlation as the forecast interval increases (Fig. 9).

A quantitative measure of forecast accuracy is the coefficient of correlation "r" between the measured and forecast time series. This is listed for the two events and locations in Table 1. The table also gives the scale factor (the slope of the line of least-squares best fit in the scatter plots in Figures 6 and 9) and the offset (the y-intercept of this line, in mm hr^{-1}). The high correlation coefficients indicate that the nowcasting algorithm is doing a good job of forecasting the pattern of reflectivity: the scale factors are close to unity and the small offsets indicate little bias in the algorithm.

Effect of catchment size

So that the effect of varying catchment area on forecast skill could be evaluated, a series of "catchments" of different areas were constructed, each centred on the Whangaparoa rainfall station. The catchments were square and oriented N-S, E-W, with sides of 1, 2, 4, 8, 16, 32, 64 and 128 km (the 1 km square "catchment" corresponding to a single radar data element).

Spatial integration over a catchment area renders the loss of the small spatial- and temporal-scale variability in the smoothed forecasts less significant. For the calculated measures of forecast skill, it reduces the influence of these small scales in the measured reflectivity and also reduces the effect of timing and positioning errors in the forecast. Increasing the catchment area therefore tends to improve the correlation between observed and forecast reflectivity (Fig. 10). The effect of varying catchment area is also seen in the measured versus forecast scatter diagrams and correlation coefficients (Fig. 11).

The improvement in accuracy with increasing catchment area reflects a major strength of radar measurements of precipitation. Precipitation, as well as having

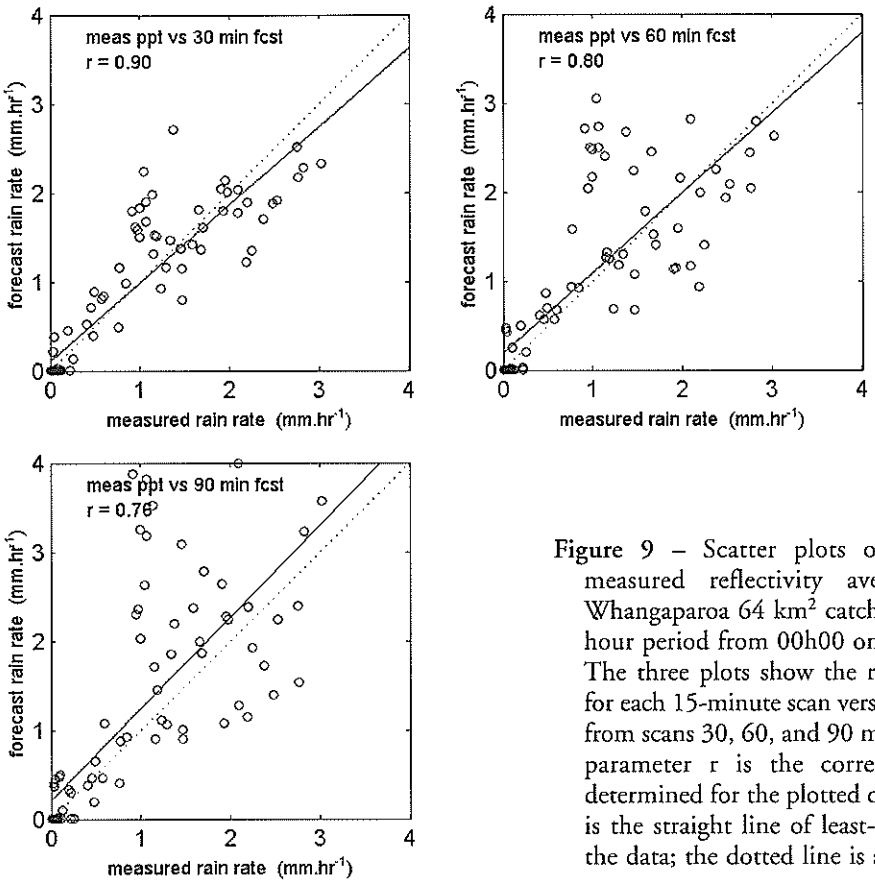

Figure 9 – Scatter plots of forecast versus measured reflectivity averaged over the Whangaparoa 64 km^2 catchment, for the 24-hour period from 00h00 on 18 August 1998. The three plots show the rain rate measured for each 15-minute scan versus the rate forecast from scans 30, 60, and 90 minutes earlier. The parameter r is the correlation coefficient determined for the plotted data. The solid line is the straight line of least-squares best fit to the data; the dotted line is a 1:1 line.

Table 1 – Correlation coefficient r, scale factor and offset (see text) for the time series of measured-forecast reflectivity pairs, for the two storms and two catchments: (i) Mahurangi catchment, 06h00 on 30 June to 05h45 on 01 July, (ii) Whangaparoa 64 km^2 catchment, 06h00 on 30 June to 05h45 on 01 July, (iii) Mahurangi catchment, 00h00 to 23h45 on 18 August, (iv) Whangaparoa 64 km^2 catchment, 00h00 to 23h45 on 18 August.

	Mahu 30 June			Whanga 30 June			Mahu 18 August			Whanga 18 August		
Fcast period	**r**	**scale**	**offset**	**r**	**scale**	**offset**	**r**	**scale**	**offset**	**r**	**scale**	**offset**
30	0.88	1.02	0.01	0.80	0.77	0.04	0.84	0.99	0.02	0.90	0.88	0.11
60	0.83	1.02	0.03	0.75	0.81	0.06	0.81	1.22	0.02	0.81	0.91	0.17
90	0.80	0.91	0.06	0.74	0.82	0.07	0.78	1.40	0.01	0.76	1.05	0.18

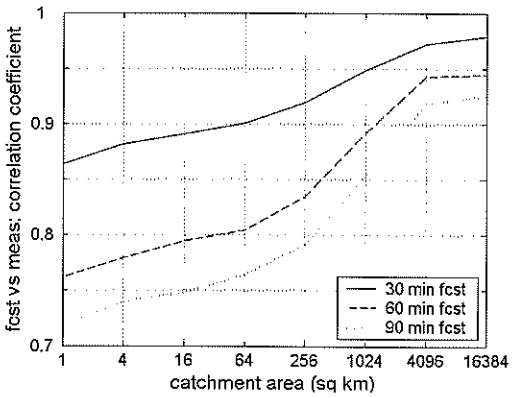

Figure 10 – The effect of catchment area on the measured/forecast correlation coefficients. Data are from the Whangaparoa area, for the second (18 August 98) event, and for forecast periods of 30, 60, and 90 minutes.

a reflectivity that fluctuates in time for a particular sampled volume, is also generally highly variable spatially over a catchment. Spatially integrated estimates, which are possible using radar data, average out this variability. While these estimates are still subject to errors in estimating the precipitation from the measured reflectivity, they are nonetheless often more accurate than estimates based on areal extrapolation from point measurements made by rain gauges, which may be accurate measurements of rainfall but are only locally valid.

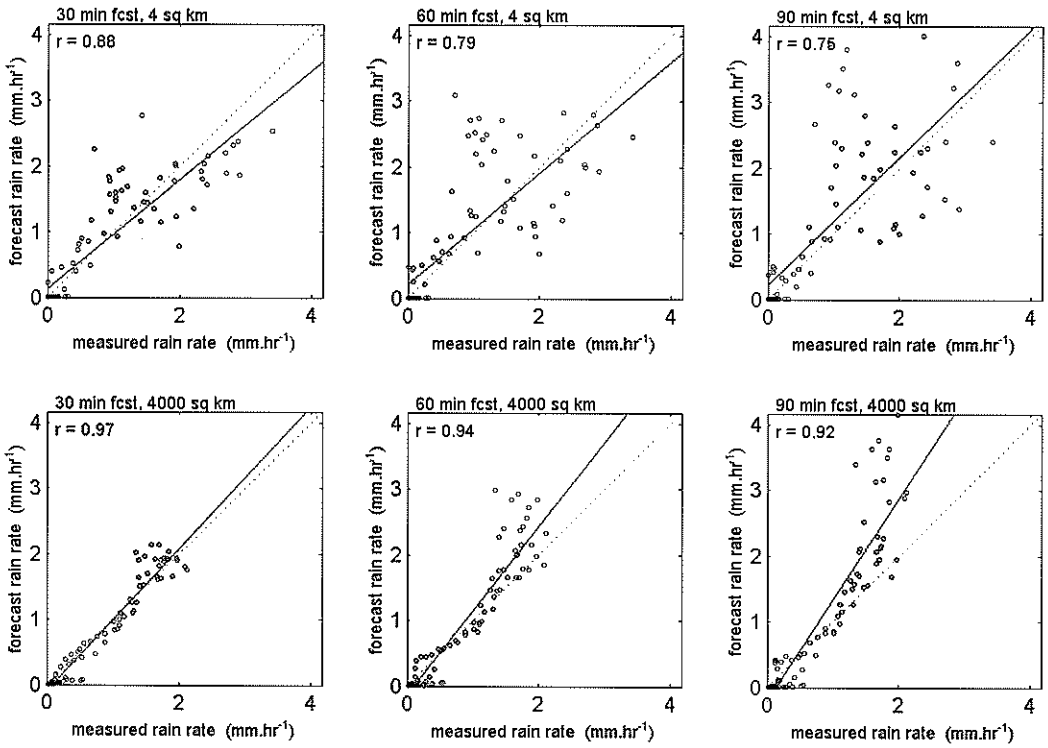

Figure 11 – Scatter plots of measured versus forecast rain rate for Whangaparoa, 00h00 to 23h45 on 18 August, for (left to right) 30, 60 and 90 minute forecasts, for 4 km^2 (upper) and 4000 km^2 (lower) catchment areas.

Accuracy and skill

The coefficient of correlation, scale factor and offset are reasonable measures of accuracy and allow the effects of changes in the algorithm and of various permutations of forecast period, catchment area and so on to be compared, but they do not directly indicate whether the nowcast algorithm displays forecast skill, i.e. offers any improvement or advantage over a forecast made without the exercise of any skill. A simple indication of skill can be gained by comparing the results for one case with what might have been forecast had we assumed the initial reflectivity simply persisted.

For the 64 km^2 Whangaparoa catchment, the correlation coefficient between the measured rain rate and the nowcast rain rate is given in Table 2 for forecast periods of 30, 60 and 90 minutes. Also given is the correlation coefficient between the measured rain rate and persistence forecasts—not the nowcasts made 30, 60 and 90 minutes earlier but the rain rates that were actually measured at those earlier times. These would correspond to forecasts made at the earlier time if the forecasts had been made by assuming that the measured rain rates simply persisted, unchanged in position and intensity. The fourth column is a skill score obtained using the relationship:

$$skill = \frac{(r_n - r_p)}{(1 - r_p)} \times 100\%$$

where $(r_n - r_p)$ represents the improvement in accuracy of the nowcast over persistence and $(1 - r_p)$ the maximum potential improvement, perfect accuracy over persistence.

The results show that the errors in forecasting the precipitation reflectivity are approximately halved when the nowcasting algorithm is used in place of persistence as the forecast method.

Table 2 – Correlation coefficient r for nowcast and persistence forecasts, and skill score (see text), for the 24-hour period 06h00 on 30 June to 06h00 on 01 July 1998, for the Whangaparoa 64 km^2 catchment.

Forecast period	r nowcast	r persistence	Skill (%)
30	0.800	0.694	34.6
60	0.741	0.386	57.9
90	0.729	0.256	63.6

Conclusions

The recently developed nowcasting algorithm described here can provide short-term precipitation forecasts using data from the MetService NZ weather radars. The algorithm has been shown to provide a good level of accuracy for forecast periods of up to 90 minutes, in two case studies of frontal precipitation in areas of the Auckland region, using data from the winter of 1998. It offers an improvement over persistence forecasts and opens up the opportunity to extend the forecast period for hydrological forecasts by over an hour.

Further testing of the algorithm is underway, using comparisons with catchment flow data and using a revised algorithm that allows independent translation vectors for each quadrant, to provide for rotation as well as translation of the forecast field.

Acknowledgements

The work has been supported by the Foundation for Research, Science and Technology under contract C01X0014. We are grateful to the Dr Alan Seed, Bureau of Meteorology, Melbourne, Australia, for his help in implementing the nowcasting algorithm. We also thank Metservice (NZ) for the supply of the radar data.

References

Austin, G.L; Bellon, A. 1974: The use of digital weather records for short-term precipitation forecasting. *Quarterly Journal of the Royal Meteorological Society 100(426)*: 658-664.

Austin, P.M. 1987: Relationship between measured radar reflectivity and surface rainfall. *Monthly Weather Review 115(5)*: 1053-1071.

Bellon, A.; Lovejoy, S.; Austin, G.L. 1980: Combining satellite and radar data for the short-range forecasting of precipitation. *Monthly Weather Review 108(10)*: 1554-1566.

Bremaud, P.J.; Pointin, Y.B. 1993: Forecasting heavy rain from raincell motion using radar data. *Journal of Hydrology142(1-4)*: 373-389.

Kessler, E.; Russo, J.A. 1963: Statistical properties of weather radar echoes. Preprints, 10th Weather Radar Conference, Washington, D.C., American Meteorological Society, 25-33.

Ligda, M.G. 1953: The horizontal motion of small precipitation areas as observed by radar. MIT Technical Report 21, Department of Meteorology, Cambridge, MA, p. 60.

Marshal, J.S.; Palmer, W.M.K. 1948: The distribution of raindrops with size. *Journal of Meteorology 5(4)*: 165-166.

Mecklenburg, S.; Joss, J.; Schmid, W. 2000: Improving the nowcasting of precipitation in an Alpine region with an enhanced radar echo tracking algorithm. *Journal of Hydrology 239(1-4)*: 46–68.

Pierce, C.E.; Hardaker, P.J.; Collier, C.G.; Haggett , C.M. 2000: GANDOLF: a system for generating automated nowcasts of convective precipitation. *Meteorological Applications 7(4)*: 341-360.

Seed, A.W. 2001: A dynamic and spatial scaling approach to advection forecasting. Proceedings of the 30th International Conference of Radar Meteorology, Munich, 19-24 July 2001, American Meteorological Society, 492-494.

Seed, A.W. 2003: A dynamic and spatial scaling approach to advection forecasting. *Journal of Applied Meteorology 42(3)*: 381-388.

Smith, K.T.; Austin, G.L. 2000: Nowcasting precipitation – a proposal for a way forward. *Journal of Hydrology 239(1-4)*: 34–45.

Wilson, J.W.; Crook, N.A.; Mueller, C.K.; Sun, J.; Dixon, M. 1998: Nowcasting thunderstorms: a status report. *Bulletin of the American Meteorological Society 79(10)*: 2079-2099.

Manuscript received 7 March 2003; accepted for publication 19 July 2003